

Activated carbon fibres prepared from kenaf: influence of the experimental conditions on the morphology and textural properties

Eduardo M. Cuerda-Correa^{1,*}, Vicente Gómez-Serrano¹, A. Macías-García², J. Valente-Nabais³ and P. J. M. Carrott³

¹Dept. of Inorganic Chemistry, Faculty of Sciences, University of Extremadura, Avda de Elvas s/n, Badajoz, SPAIN. E-06071

²Dept. of Materials Science, School of Industrial Engineering, University of Extremadura, Avda de Elvas s/n, Badajoz, SPAIN. E-06071

³Dept. of Chemistry, Faculty of Sciences, University of Évora, Rua Romão Ramalho, 59, Évora, PORTUGAL. 7000-671

Email: emcc@unex.es

Keywords

(carbon fibres, gasification, microstructure)

INTRODUCTION

Porous materials are usually heterogeneous both structurally and energetically. Activated carbon fibres (ACFs) are relatively novel fibrous adsorbents produced for example from pith, cellulose, lignocellulose, phenol resin and polyacrylonitrile (Peebles, 1995; Ryu, 1999). ACFs show important advantages with respect to conventional activated carbons. Among these advantages it is worth noting their high adsorption capacity and easiness to handle. Their main inconvenience lays on the difficulty of choosing adequate activating agents and activation conditions that are required in order to maintain the fibrous morphology.

The adsorption capacity of ACFs depends on many factors, such as raw materials, activation process, pore structure and surface functionalities (Suffet, 1981; Park, 1999). Surface roughness is an important factor that influences the adsorption properties of an activated carbon. Fractal dimension is a measure of roughness of a surface. The use of the fractal concept is becoming very popular as a tool to characterize the texture of complex materials, such as porous solids. The fractal properties of these porous systems were determined by means of several techniques such as gas adsorption, mercury porosimetry and Small-Angle X-Ray Scattering (SAXS and SANS).

Kenaf is an herbaceous annual plant that belongs to the family of *Malvaceae*. Kenaf possesses both, long and short fibre. The aim of this work is to study the influence of the preparation conditions on the fractal dimension and porous texture of ACFs prepared from long fibres of kenaf by physical activation using carbon dioxide as activating agent.

* Author to whom any correspondence should be addressed.

EXPERIMENTAL

Preparation of the samples

The precursor used for the production of ACFs was kenaf. A Termolab tubular furnace provided with Eurotherm 904 temperature controllers and a 1 m long tubular ceramic insert was used. The internal temperature of the furnace was first calibrated and the length and position of the constant temperature hot zone determined. About 1.5 g of kenaf fibre were placed in a 10 cm stainless steel boat with perforated ends to facilitate gas flow and positioned in the centre of the constant temperature zone. The carbonisation of the samples was carried out at 300 and 400°C. The heating rate used was 5°C min⁻¹ under a constant N₂ flow of 85 cm³ min⁻¹. The isothermal carbonisation time was 0.5 or 1 h (see Table 1). The carbonised sample showing optimal characteristics in terms of porosity and surface area was selected as precursor for the preparation of the activated fibres. The activation temperatures were 500, 600 and 700°C. A flow of activating agent (carbon dioxide) equal to 85 cm³ min⁻¹ was used, the heating rate being 5°C min⁻¹. The isothermal activation time was 2 or 4 h (see Table 1). Once the isothermal activation time had finished, the activating agent flow was replaced by a N₂ flow and the furnace was cooled to a final temperature of 50°C. Next, the sample was removed from the oven and kept in a tightly closed container.

TABLE 1: Nomenclature and preparation conditions of the different samples.

Sample	Carbonisation temperature (°C)	Carbonisation time (h)	Activation temperature (°C)	Activation time (h)
CF3-05	300	0.5	-	-
CF4-05	400	0.5	-	-
CF3-1	300	1	-	-
CF4-1	400	1	-	-
ACF5-2	400	0.5	500	2
ACF5-4	400	0.5	500	4
ACF6-2	400	0.5	600	2
ACF6-4	400	0.5	600	4
ACF7-2	400	0.5	700	2
ACF7-4	400	0.5	700	4

Characterisation of the samples

The samples were texturally characterised by gas adsorption (N₂, 77 K), mercury porosimetry and scanning electron microscopy (SEM). Adsorption isotherms of N₂ (purity > 99.998%) at 77 K were determined using an adsorption apparatus (Autosorb-1, Quantachrome). Adsorbents were placed in a glass container and degassed at 10⁻³ Torr at 120°C overnight prior to the adsorption measurements. A Quantachrome porosimeter, Autoscan-60, was used to obtain the mercury intrusion curves. The values of surface tension and contact angle used in the computational program of the porosimeter were 0.480 N m⁻¹ and 140°, respectively. The sample morphology was observed using a scanning electron microscope (SEM; model S-3600N, Hitachi, Japan). The specimens for SEM observation were prepared by depositing the fibres onto specimen-stubs with conductive double-sticky copper tapes, and then sputter-coating (model Polaron SC7640, Quorum Technologies Ltd, U.K.) the fibre surfaces with Au-Pd to prevent electrical charging during examination. Imaging was done in the high vacuum mode at an accelerating voltage of 20 kV, using secondary electrons.

The fractal dimension is often used as an index of roughness or irregularity of the surface (Pérez-Bernal, 2000; Diduszko, 2000). Recently, several researchers reported the fractal dimension of activated carbon (Gauden, 2001; Hayashi, 2002). In this study, the fractal dimension was determined by applying the following Frenkel-Halsey-Hill (FHH) equation (Halsey, 1948) to the N₂ adsorption data (Kaneko, 1991):

$$\frac{q}{q_e} = K \left[\frac{1}{P} \left(\frac{P_0}{P} \right)^{\frac{1}{D-3}} \right]^{(D-3)} \quad [1]$$

where q is the amount adsorbed at equilibrium pressure, P ; q_e is the amount adsorbed filling micropore volume; P_0 is saturated pressure; K is a constant; D is the fractal dimension. Thus, the plot of $\ln q$ vs $\ln(\ln(P_0/P))$ shows linear trend and the slope ($D-3$) may be used to calculate the fractal dimension, D .

According to the referred authors, a perfectly smooth surface has the fractal dimension of 2, whereas a very rough or irregular surface has the fractal dimension of 3.

Mercury porosimetry is based on the intrusion of pores by mercury as a certain pressure is applied; increasing pressure makes smaller pores accessible to mercury. For pore wall surface in general it was shown (Pfeifer, 1987) that the pore size distribution function, $-dV/dr$, could be expressed as

$$-\frac{d}{dr} \frac{V}{r} = k_1 r^{-D} \quad [2]$$

where k_1 is a proportionality constant and P is the applied pressure. Taking logarithms yields

$$\ln \left(\frac{d}{dr} \frac{V}{r} \right) = \ln k_1 - (D-1) \ln P \quad [3]$$

Hence, D values can be derived from the slope of $\log(dV/dr)$ versus $\log(P)$ plots. Smooth surfaces ($D=2$) would present slopes close to -2 whereas rougher surfaces (for which D approaches 3) would present slopes approaching -1.

RESULTS AND DISCUSSION

Carbonisation of the kenaf fibres

Previous thermogravimetric analyses of the kenaf fibres (not shown here for the sake of brevity) suggest that the carbonisation should not be carried out at temperatures above 400°C, since significant weight losses are observed. Consequently, two thermal treatment temperatures namely 300 and 400°C were chosen for the carbonisation of the kenaf fibres.

The adsorption isotherms of N₂ at 77 K were registered for the carbonised samples. By application of the BET and Dubinin-Radushkevich equations to the adsorption data the values of the specific surface area (S_{BET}) and micropore volume (V_{D-R}), respectively, were calculated. Such values are listed in Table 2. From the results obtained it may be observed that the specific surface area of the

sample CF4-05 reaches $29 \text{ m}^2 \text{ g}^{-1}$. Such value is higher than those reported by other authors regarding different fibres heated at higher carbonisation temperatures (Ryu, 1999). When the thermal treatment time increases the value of S_{BET} decreases from $29 \text{ m}^2 \text{ g}^{-1}$ to $3 \text{ m}^2 \text{ g}^{-1}$. This fact may be due to a more remarkable shrinkage of the carbonaceous structure at longer carbonisation times.

TABLE 2: Textural properties and fractal dimensions of the different samples.

Sample	$S_{\text{BET}} (\text{m}^2 \text{ g}^{-1})$	$V_{\text{D-R}} (\text{cm}^3 \text{ g}^{-1})$	$V_{\text{me}} (\text{cm}^3 \text{ g}^{-1})$	$V_{\text{ma}} (\text{cm}^3 \text{ g}^{-1})$	D_{FHH}	D_{P}
CF3-05	8	0.005	0.010	0.021	2.37	2.35
CF4-05	29	0.016	0.031	0.034	2.43	2.48
CF3-1	3	0.001	0.009	0.017	2.03	2.16
CF4-1	3	0.001	0.010	0.028	2.27	2.30
ACF5-2	21	0.012	0.020	0.036	2.56	2.62
ACF5-4	7	0.004	0.006	0.040	2.49	2.64
ACF6-2	33	0.016	0.024	0.048	2.78	2.80
ACF6-4	8	0.005	0.092	0.060	2.60	2.84
ACF7-2	341	0.181	0.154	0.021	2.54	2.48
ACF7-4	1031	0.551	0.501	0.018	2.50	2.49

The meso- and macropore volumes (V_{me} and V_{ma} , respectively) were determined from the mercury porosimetry experiments and are also listed in Table 2. Such values indicate that the narrowest average pore size as well as the most developed porous texture correspond to sample CF4-05.

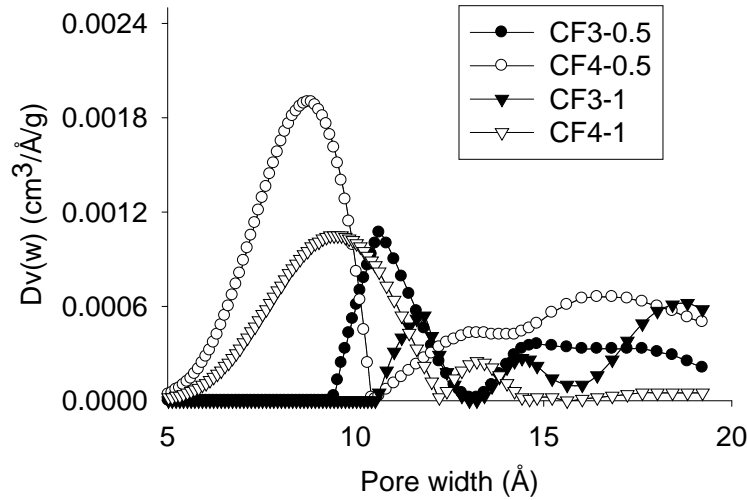


FIGURE 1: Pore size distributions of the carbonised samples

The creation of micropores increases markedly when the carbonisation was carried out at 400°C (see Figure 1). Because of the creation of smaller pores in the fibres, this reaction leads to an increase in surface area as shown in Table 2. Furthermore, the micropore volume decreases (CF4-05, $V_{\text{mi}} = 0.016 \text{ cm}^3 \text{ g}^{-1} > \text{CF4-1, } V_{\text{mi}} = 0.001 \text{ cm}^3 \text{ g}^{-1}$) as the treatment time increases. Figure 1 illustrates the pore size distribution of the carbonised samples. In this Figure it may be observed that the average pore size becomes larger as the carbonisation time grows. This trend may be due to the fact that, as the treatment time increases, the narrow pores may establish connections and finally combine, thus giving rise to larger pores and to a subsequent decrease of the micropore volume.

This hypothesis is corroborated from the results of the fractal dimensions of the different samples that are listed in Table 2. As the treatment time of the carbonised samples increases, the values of D calculated from the adsorption isotherms (D_{FHH} , corresponding to narrow pores) as well as those calculated from the mercury porosimetry (D_P , corresponding to wider pores) decrease. This trend points out that the surface irregularities are less remarkable when the treatment time is relatively long.

Activation of the kenaf fibres

Influence of the activation temperature

Table 2 clearly shows that, for a treatment time equal to 2 h, the variation of S_{BET} is not remarkable at low temperatures (ACF5-2, $21 \text{ m}^2 \text{ g}^{-1}$; ACF6-2, $33 \text{ m}^2 \text{ g}^{-1}$) whereas it noticeably increases at higher temperatures (i.e., 700°C ; ACF7-2, $341 \text{ m}^2 \text{ g}^{-1}$). The same trend is observed for the samples prepared using a the treatment time of 4 h. In this latter case, the values of S_{BET} are even lower for samples prepared at 500 and 600°C and higher for that prepared at 700°C (ACF7-4, $1031 \text{ m}^2 \text{ g}^{-1}$). These results suggest that when the activation temperature is relatively low the pores are blocked or occluded due to the presence of pyrolysis products. Such products are eliminated at higher temperatures (i.e., 700°C), when the gasification processes are predominant. As a consequence, the pores are cleaned and the textural properties of the products are improved. It is worth noting that these results are better than those previously reported in the literature for similar ACFs (Ko, 1992) and in the present study lower carbonisation and activation temperatures have been used.

The changes in porosity follow a similar trend, the pore volume increasing as temperature does, excepting V_{ma} corresponding to sample ACF7-2. The same behaviour is observed for the fractal dimensions. This variation pattern suggests that the surface irregularity decreases markedly when the activation temperature reaches 700°C . As indicated above, this fact may be due to the opening of blocked pores as well as to the connection or joining of small pores that gives rise to larger ones when the activation temperature rises up to 700°C . Thus, in figure 2 it may be observed that the pores size distribution shows an open ending, which is indicative of the presence of large pores with diameters close to those corresponding to the mesopores.

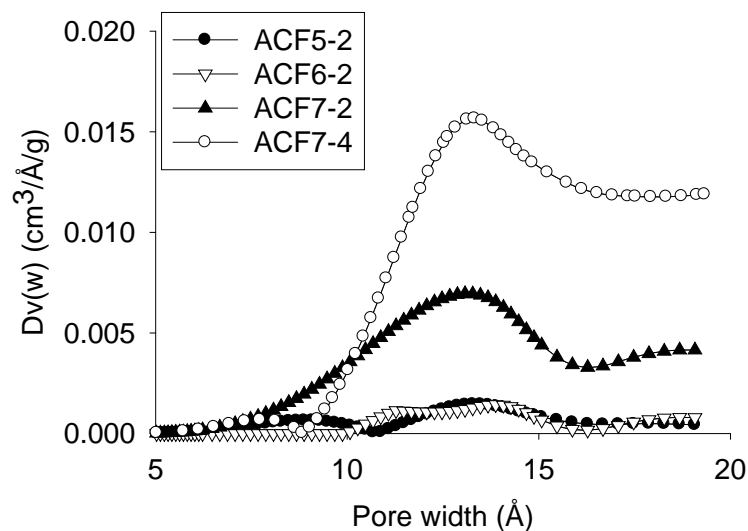


FIGURE 2: Pore size distributions of the activated samples

This trend is observed again when the fractal dimension, D , is determined. This fact suggests that, for sample ACF7-2, the surface irregularities decrease noticeably. The values of the fractal dimension vary in a similar manner to that described in the previous paragraph. This may be indicative of the fact that, as temperature rises, the thermal treatment and the presence of activating agent (i.e., carbon dioxide) favour the porous development of the samples. As a consequence, the surface irregularity is more remarkable and D increases. This trend, again, is broken when the thermal treatment is carried out at 700°C. This could be indicative of the presence of pores that show a less irregular surface.

Influence of the activation time

As indicated previously, two well-differentiated trends are observed depending on the treatment temperature. Thus, at low temperatures (i.e., 500-600°C) as the treatment time increases a decrease in both specific surface area and micropore volume is observed whereas the wider pores (i.e., meso and macropores) increase in volume. This latter fact corroborates the decrease of the D values, probably due to the opening of previously blocked pores as well as to the development of larger pores as a consequence of the interconnection of narrower ones. The occurrence of new larger pores would lead to a decrease in the surface heterogeneity of the samples and, therefore, to lower values of D .

On the other hand, the samples prepared at 700°C show an increase in all the textural parameters excepting the macropore volume and the fractal dimension (see table 2). This trend is clearly shown in figure 2. In this figure it may be easily observed that the final portion of the pore size distribution plots of the activated samples points out the presence of large micropores with a pore diameter close to that corresponding to the mesopores. The origin of these pores would be related to the same phenomena indicated in the previous paragraph (i.e., opening of blocked pores and interconnections). As a consequence, the macropore volume and the fractal dimension of the samples would decrease. This hypothesis is illustrated by the SEM images of samples ACF7-2 (figure 3, left) and ACF7-4 (figure 3, right). In both images it may be observed that, in addition to the interconnection and opening of pores, a detachment of the external layers of the pores takes place, which leads to more homogeneous pores with smoother surfaces and, consequently, to lower values of D .

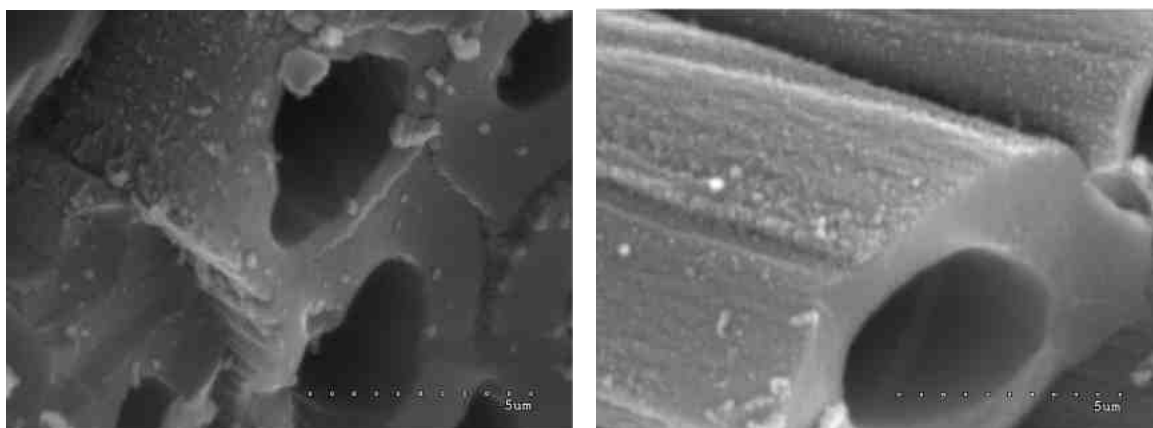


FIGURE 3: SEM images of samples ACF7-2 (left) and ACF7-4 (right)

CONCLUDING REMARKS

The specific surface area of the sample carbonised at 400°C for 0.5 h is higher than other values previously reported in the literature. When the treatment time increases, the value of S_{BET} decreases markedly, due to the development of defects between the basal planes of the fibre. Moreover, long treatment times exert a negative effect on the porous development of the samples in terms of micropore volume and fractal dimension. On the other hand, the activation time does not influence the specific surface area of the samples prepared at low temperatures. On the contrary, for samples activated at 700°C the porous texture is strongly developed, especially when the samples are activated for 4 h. The same trend is observed for the pore volumes and fractal dimension of these latter samples. Finally, the SEM images suggest that the development of pores in the activated samples makes it possible to use kenaf fibres as precursor for potential applications in fields such as electronics. In this connection, further experiments are being carried out with promising results.

Acknowledgements

The authors gratefully acknowledge financial support provided by the Spanish Ministry of Environment through the Research Project 210/2004/3.

References

- Diduszko, R., Swiatkowski, A. and Trznadel B. J. (2000). On surface of micropores and fractal dimension of activated carbon determined on the basis of adsorption and SAXS investigations. *Carbon*, **38**, 1153-1162.
- Gauden, P. A., Terzyk, A. P. and Rychlicki, G. (2001). The new correlation between microporosity of strictly microporous activated carbons and fractal dimension on the basis of the Polanyi–Dubinin theory of adsorption. *Carbon*, **39**, 267-278.
- Halsey, G.D. (1948) Physical adsorption on non-uniform surfaces. *J. Chem. Phys.*, **16**, 931-937.
- Hayashi, J., Horikawa T., Muroyama, K. and Gomes V. G. (2002). Activated carbon from chickpea husk by chemical activation with K_2CO_3 : preparation and characterization. *Micropor. Mesopor. Mat.*, **55**, 63–68.
- Kaneko K., Sato M., Suzuki T., Fujiwara Y., Nishikawa K. and Jaroniec M. (1991) Surface fractal dimension of microporous carbon fibres by nitrogen adsorption *J. Chem. Soc. Faraday Trans.*, **87**, 179-184.
- Ko, T.H., Chiranairadul, P., Lu, C.K, and Lin, C. H. (1992) The effects of activation by carbon dioxide on mechanical properties and structure of pan-based activated carbon fibers. *Carbon*, **30**, 647-655.
- Park, S. J. and Kim, K. D. (1999). Adsorption behaviors of CO_2 and NH_3 on chemically surface-treated activated carbons. *J. Colloid Interf. Sci.*, **212**, 186-189.
- Pérez-Bernal, J. L. and Bello-López, M. A. (2000) The fractal dimension of stone pore surface as weathering descriptor. *Appl. Surf. Sci.*, **161**, 47-53.
- Peebles, L.H. (1995) Carbon Fibers: Formation, Structure and Properties, CRC Press, Boca Raton.
- Pfeifer, P. (1987) Characterization of surface irregularity. *Preparative Chemistry Using Supported Reagents* (Ed. P. Laszlo). Academic Press, New York.
- Ryu, Z., Zheng, J., Wang, M. and Zhang, B. (1999). Characterization of pore size distributions on carbonaceous adsorbents by DFT. *Carbon*, **37**, 1257-1264.
- Suffet, Y. H. and McGuire, M. J. (1981). Activated Carbon Adsorption, Ann Arbor Science, Michigan.